Rev. Adv. Mater. Sci. 43 (2015) 38-44

# PLASTIC DEFORMATION THROUGH DETWINNING AND ITS EFFECT ON ELECTRIC RESISTIVITY IN ULTRAFINE-GRAINED METALS WITH NANOTWINNED STRUCTURES

**I.A. Ovid'ko[1,2,3], N.V. Skiba[1,2,3] and A.G. Sheinerman[1,2,3]**

[1]Research Laboratory for Mechanics of New Nanomaterials,
Peter the Great St. Petersburg Polytechnical University, St. Petersburg 195251, Russia
[2]Department of Mathematics and Mechanics, St. Petersburg State University, St. Petersburg 198504, Russia
[3]Institute of Problems of Mechanical Engineering, Russian Academy of Sciences,
St. Petersburg 199178, Russia

*Received: September 10, 2015*

**Abstract.** A theoretical model is suggested which describes plastic deformation through detwinning processes in ultrafine-grained metallic materials containing high-density ensembles of nanoscale twins within grains (nanotwinned metals). In the framework of the suggested model, detwinning occurs via stress-driven migration of incoherent boundaries of nanoscale twins. The energy and stress characteristics of the detwinning processes in nanotwinned metals with face-centered cubic lattices are calculated. Our theoretical results are well consistent with corresponding experimental data reported in the literature. Also, the effect of the detwinning processes on the electric resistivity of nanotwinned metals is estimated.

## 1. INTRODUCTION

Ultrafine-grained metals and alloys show excellent mechanical properties that represent the subject of intensive research efforts; see, e.g., [1–10]. In recent years, particular attention has been devoted to ultrafine-grained metallic materials containing high-density ensembles of nanoscale twins within grains (hereinafter called nanotwinned metals), because of the outstanding combination of their superior strength and functional ductility at room temperature [11–19]. Besides, these materials are characterized by enhanced electrical conductivity [11]. Despite the recent progress in the research efforts addressing the unique mechanical properties of nanotwinned metals, the micromechanisms/modes of plastic deformation in these metals are not fully understood and represent the subject of intensive discussions; see, e.g., [11–24]. So, the specific deformation modes operating in nanotwinned metals are conventionally treated to be lattice dislocation slip hampered by twin boundaries and plastic deformation occurring through migration of coherent twin boundaries (CTBs) [11–24]. In general, however, with the specific structural features of nanotwinned metals, other deformation modes can come into play in such metals. In particular, the presence of high-density ensembles of nanoscale twins within grains in nanotwinned metals admits plastic flow through transformations of twins, which are different from CTB migration. For example, recently, using transmission electron microscopy, several research groups observed detwinning of nanotwinned Cu occurring via migration of incoherent twin boundaries (ITBs) under indenter loading [25–29]. In particular, Liu et al. [27,29] observed

Corresponding author: I.A. Ovid'ko, e-mail: ovidko@nano.ipme.ru

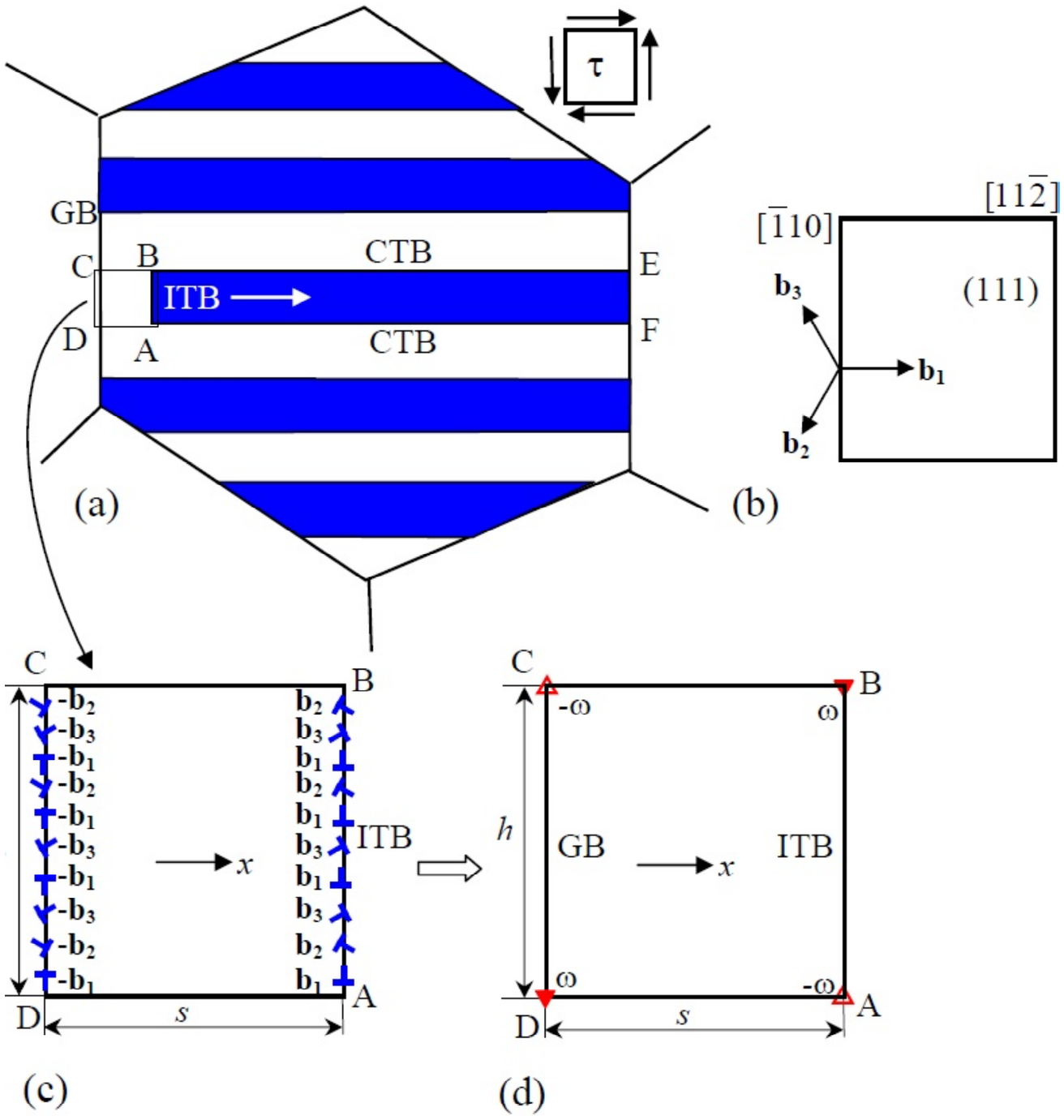


**Fig. 1.** (Color online) Detwinning in a deformed nanotwinned solid. (a) A model grain of a nanotwinned solid under the action of an applied shear stress $\tau$. An incoherent twin boundary (ITB) nucleates at a grain boundary and moves under the action of the applied shear stress along coherent twin boundaries (CTBs). (b) Geometry of dislocations composing the ITB. (c) A magnified region ABCD of figure (a) shows a dislocation ensemble at the ITB and an ensemble of opposite-sign dislocations at the grain boundary. (d) The dislocation structure shown in figure (c) is approximated as a quadrupole of wedge disclinations specified by the strengths $\pm\omega$.

migration of an ITB with the length of 5.5 nm in nanotwinned Cu at ultralow indentation stress of 0.1 GPa, well below the stress needed for macroscopic yielding. Wang et al. [25], using molecular dynamics simulations, confirmed that in the case of ultrathin twins with a thickness below 2 nm, ITB migration can proceed at low shear stresses below 0.3 GPa. At the same time, the reasons for easy detwinning of thin twins in nanotwinned Cu are not yet fully understood, and the relations of the critical stress for detwinning of nanotwinned metals (through ITB migration) with the twin thickness and ITB structure have not been revealed. The main aims of this paper are to suggest a theoretical model that describes the detwinning processes in nanotwinned metals having face-centered cubic (fcc) lattices and to calculate the critical parameters for the onset of detwinning in such metals. Also, the effect of detwinning processes on the electric resistivity of nanotwinned metals is estimated.

## 2. DETWINNING THROUGH THE FORMATION AND MOTION OF INCOHERENT TWIN BOUNDARIES IN NANOTWINNED FACE-CENTERED CUBIC METALS. MODEL

Let us consider a model grain in a deformed nanotwinned metal with a face-centered cubic (fcc) lattice (Fig. 1a). Within our model, the grain is composed of growth twins divided by CTBs. We assume that an applied shear stress $\tau$ acts in the examined grain as shown in Fig. 1a. In the initial state, the model grain contains a rectangular twin CEFD bounded by grain boundary (GB) segments CD and EF and CTB CE and BF. We consider the situation where an ITB AB is generated at the GB segment CD and moves along the CTBs CE and DF (Fig. 1a). In doing so, the motion of the ITB AB is accompanied by the disappearance of the CTB fragments

AD and BC, thus leading to the shrinking of the twin AFEB. If the ITB approaches the GB EF, the twin AFEB completely disappears, thus promoting local detwinning in the nanotwinned solid.

We now consider the geometry of the formation and motion of the ITB AB. It is known that, in fcc solids, CTBs are located at {111} crystal planes, while ITBs commonly lie in {112} planes. For definiteness, we suppose that CTBs AF and BE occupy (111) crystal planes, while the ITB AB is located at a $(11\bar{2})$ crystal plane. Within our model, the formation and motion of the $(11\bar{2})$ ITB (accompanied by the shrinkage of the CTBs BE and AF) can be realized by the formation and simultaneous motion of the Shockley partial dislocations along all the (111) planes of the twin CEFD [25,26]. Each Shockley partial has the line direction $[\bar{1}10]$ and the Burgers vector $\boldsymbol{b}_1$, $\boldsymbol{b}_2$ or $\boldsymbol{b}_3$, where $\mathbf{b}_1 = (a/6)[11\bar{2}]$, $\mathbf{b}_2 = (a/6)[1\bar{2}1]$ and $\mathbf{b}_3 = (a/6)[\bar{2}11]$ (Fig. 1b), with $a$ being the crystal lattice parameter. The dislocations specified by the Burgers vector $\boldsymbol{b}_1$ represent edge dislocations, while those with the Burgers vectors $\boldsymbol{b}_2$ and $\boldsymbol{b}_3$ are 30° mixed dislocations. The vector sum of the three Burgers vectors $\boldsymbol{b}_1$, $\boldsymbol{b}_2$, and $\boldsymbol{b}_3$ is zero, that is, $\boldsymbol{b}_1+\boldsymbol{b}_2+\boldsymbol{b}_3=0$.

Due to the conservation of the dislocation Burgers vector, each nucleating dislocation with the Burgers vector $\boldsymbol{b}_k$ (where $k$ = 1,2,3) should leave the opposite-sign dislocation with the Burgers vector $-\boldsymbol{b}_k$ at the GB fragment CD (Fig. 1c). Thus, the generation and motion of the ITB CD can be realized by the formation of the dipoles of the dislocations with the Burgers vectors $\pm\boldsymbol{b}_k$ at each (111) plane, followed by the simultaneous motion of the dislocations with the Burgers vectors $\boldsymbol{b}_k$ that form the ITB AB (Fig. 1c).

In general, the dislocations with the Burgers vectors $\boldsymbol{b}_k$ can produce both tilt and twist misorientations. Let us denote the fractions of the dislocations specified by the Burgers vectors $\boldsymbol{b}_1$, $\boldsymbol{b}_2$, and $\boldsymbol{b}_3$ as $f_1$, $f_2$, and $f_3$, respectively ($f_1 + f_2 + f_3 = 1$). For simplicity, in the following, we consider the most energetically favored ITB with the misorientations on the large-scale level being constant along the boundary. Also, since screw dislocations do not interact with the shear stress $\tau$ and, at the same time, accumulate some self-energy, the formation of the ITB with the zero screw component of the net Burgers vector is most energetically favored. For definiteness, in the following, we consider this most energetically favorable case where the screw component $B_s$ of the total Burgers vector of all the dislocations composing the ITB is equal to zero, that is, $B_s = 0$. (The latter relation is realized, if $f_2 = f_3$.) In the examined case, the ITB represents a tilt boundary. In this situation, for the calculation of the self-energies that characterize the dislocation walls, the two dislocation arrays AB and CD can be approximated as a quadrupole ABCD of wedge disclinations with the strengths $\pm\omega$ (Fig. 1d). The disclination strength magnitude $\omega$ is defined as $\omega = 2\arctan(B_e/(2h))$, where $B_e$ is the edge component of the total Burgers vector of all the dislocations composing the ITB AB and $h$ is the length of this boundary, equal to the thickness of the examined twin AFEB (Fig. 1). In turn, the quantity $B_e$ is calculated as $B_e=b(f_1-f_2)h/p$, where $b=a/\sqrt{6}$ is the magnitude of the dislocation Burgers vectors and $p=a/\sqrt{3}$ is the distance between the neighboring (111) crystal planes. Since $f_2=(1-f_1)/2$ and $b/p=1/\sqrt{2}$, we obtain: $B_e=(3f_1-1)h/(2\sqrt{2})$. For the case of small disclination strengths $\omega$, when $\omega << 1$, we obtain the following relation between the disclination strength $\omega$ and the fraction $f_1$ of edge dislocations in the dislocation walls: $\omega \approx B_e/h=(3f_1-1)h/(2\sqrt{2})$.

## 3. CRITICAL PARAMETERS FOR DETWINNING IN NANOTWINNED FACE-CENTERED CUBIC METALS

Let us calculate the critical parameters for detwinning in nanotwinned fcc metals. To do so, we calculate the projection $F_x$ of the force $F$ acting on the moving ITB (per unit boundary length in the direction normal to the plane of Figs. 1c and 1d). The force $F_x$ can be calculated as follows:

$$F_x = -\frac{dW_q}{dx} - (h/p)b\tau_p^e + \tau\omega h + 2\gamma_{CTB}, \qquad (1)$$

where $W_q$ is the self-energy of the disclination quadrupole (per unit disclination length), $\gamma_{CTB}$ is the specific (per unit area) energy of the CTB, $\tau_p^e = f_1\tau_{p1} + (1 - f_1)\tau_{p2}$ is the effective Peierls stress, and $\tau_{p1}$ and $\tau_{p2}$ are the Peierls stresses for the motion of the edge and mixed 30° dislocations, respectively. In the isotropic approximation, the self-energy of the disclination quadrupole is given by [30]

$$W^q = \frac{D\omega^2h^2}{2}\left[\left(1+t^2\right)\ln\left(1+t^2\right) - t^2\ln\left(t^2\right)\right], \qquad (2)$$

where $t = s/h$, $s$ is the distance between the disclination dipoles AB and CD (Fig. 1d), $D = G/[2\pi(1-\nu)]$, $G$ is the shear modulus and $\nu$ is Poisson's ratio. Substitution of (2) to (1) and account for the relation $b/p = 1/\sqrt{2}$ yield

$$F_x = \omega h\left[ -D\omega t \log\left(1+1/t^2\right) + \tau - \frac{\tau_p^e}{\sqrt{2}\omega} + \frac{2\gamma_{CTB}}{\omega h}\right]. \quad (3)$$

The minimum value $F_{min}$ of the force $F_x$ is reached at $t \approx 0.505$. For this value of $t$, we have: $t\log(1 + 1/t)^2 \approx 0.805$. To move the ITB across the twin, the force $F_x$ acting on this ITB should be positive at any value of $t$. This condition is valid, if the minimum value $F_{min}$ of the force $F_x$ is positive, that is,

$$-0.805D\omega + \tau - \frac{\tau_p^e}{\sqrt{2}\omega} + \frac{2\gamma_{CTB}}{\omega h} > 0. \quad (4)$$

Formula (4) can be rewritten as $\tau > \tau'$, where

$$\tau' = 0.805D\omega + \frac{\tau_p^e}{\sqrt{2}\omega} - \frac{2\gamma_{CTB}}{\omega h}. \quad (5)$$

In the following, we focus our examination on the case of nanotwinned Cu characterized by the following values of material parameters: $G = 48$ GPa, $\nu = 0.34$, and $\gamma_{CTB} = 24$ mJ/m$^2$ [31]. Since the exact values of the quantities $\tau_{p1}$ and $\tau_{p2}$ for Cu at room temperature are unknown, for simplicity, we put $\tau_{p1} = \tau_{p2}$=30 MPa. With the above parameter values, the dependences of the critical stress $\tau'$ on the disclination strength $\omega$ are presented in Fig. 2, for $h$ = 5 nm (a) and 2 nm (b). Fig. 2 demonstrates that, when values of $h$ are not too small, the dependences $\tau'(\omega)$ have a minimum, whereas, for sufficiently small values of $h$, $\tau'$ monotonously decreases with diminishing $\omega$. The analysis of formula (5) shows that the transition from the first to the second case occurs at $h = h_c$, where $h_c = 2\sqrt{2}\gamma_{CTB}/\tau_p^e$. For nanotwinned Cu, from the latter relation we obtain: $h_c \approx 2.2$ nm. Also, Fig. 2b demonstrates that the formation and migration of the ITB at $h < h_c$ is favored even in the situation with $\omega = 0$, corresponding to the zero net Burgers vector of the ITB. This result is well consistent with the experimental observation [26] of the motion of an ITB containing a dislocation array characterized by a zero net Burgers vector in nanotwinned Cu under indenter loading in the case of twin thickness being around 2 nm. Also, in the situation with $h < h_c$, the formation and migration of the ITB is favored even in the absence of the applied stress ($\tau$ = 0) with the proviso that the disclination strength $\omega$ is either sufficiently small or equals zero. In the latter case (where $\omega$ = 0), the driving force for the ITB migration occurs due to dis-

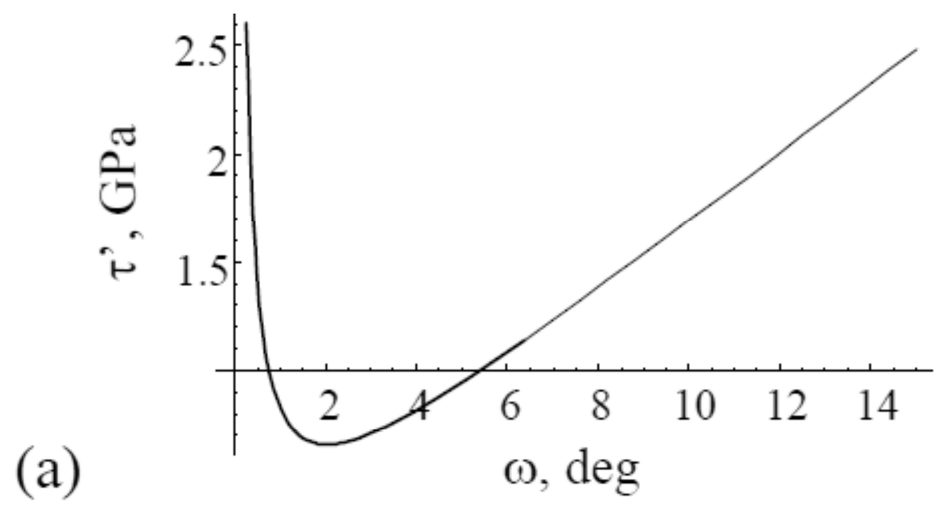


**Fig. 2.** Dependences of the critical shear stress $\tau'$ on disclination strength $\omega$ in nanotwinned Cu, for (a) $h$ = 5 nm and (b) $h$ = 2 nm.

appearance of the CTB fragments, that accompanies ITB motion.

One should bear in mind that the expression $h_c = 2\sqrt{2}\gamma_{CTB}/\tau_p^e$ for the critical twin thickness $h_c$ is obtained for the "hardest" case where all the dislocations pass the maximums of the Peierls barrier for dislocation motion simultaneously. At the same time, dislocations can overcome the maximums of the Peierls stress one by one, in which case the friction force exerted by the Peierls stress on the ITB will be lower. In the latter case, the critical thickness $h_c$ for ITB migration can be larger than $2\sqrt{2}\gamma_{CTB}/\tau_p^e$, that is, higher than 2.2 nm for Cu. This explains the experimental observation [27] of migration of an ITB with the length of 5.5 nm in nanotwinned Cu at ultra-low indentation stress of 0.1 GPa.

The equilibrium value $\omega = \omega_e$ of the disclination strength $\omega$, corresponding to the minimum at the curve $\tau'(\omega)$ at $h > h_c$ is shown in Fig. 3a as a function of the twin thickness $h$ for nanotwinned Cu. Figure 3a demonstrates that at $h > h_c$, $\omega_e$ quickly increases with rising $h$ and then approaches the nearly constant level of 2.5-3°. Using the relation $\omega \approx (3f_1 - 1)/(2\sqrt{2})$ obtained above, one can conclude that this level of $\omega$ corresponds to the values of $f_1$ (the fraction $f_1$ of edge dislocations in the dislocation wall) being around 0.38. Let us assume that the dislocation structure of the ITB can be presented as the

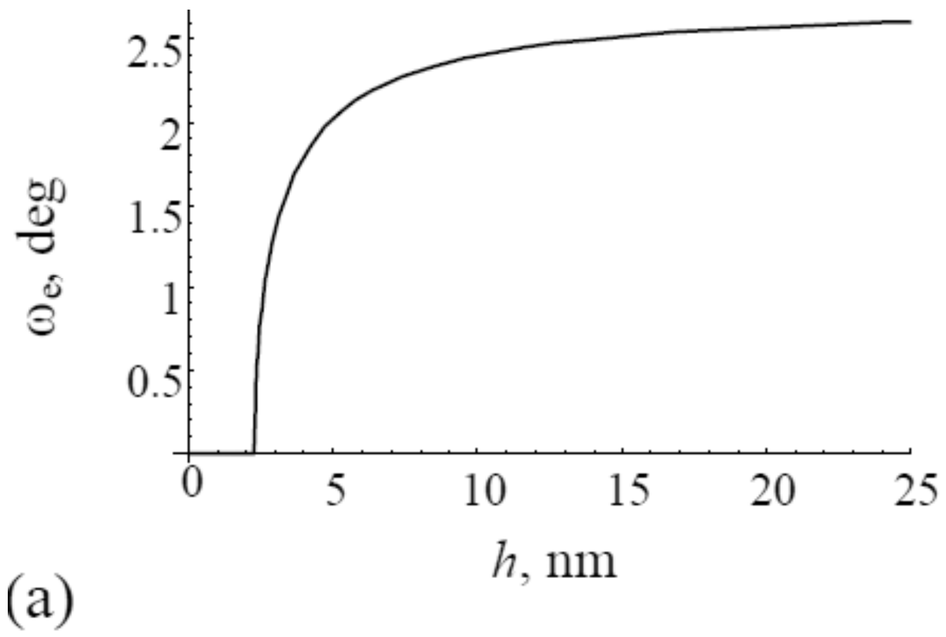


**Fig. 3.** Dependences of the equilibrium disclination strength $\omega_e$ (a) and the critical shear stress $\tau_c$ (b) on twin thickness $h$ in nanotwinned Cu.

superposition of the ITB fragments containing three adjacent dislocations with different Burgers vectors $\boldsymbol{b}_1$,$\boldsymbol{b}_2$, and $\boldsymbol{b}_3$ (which provide the zero sum Burgers vector of each such ITB fragment) and the ITB fragments containing two adjacent dislocations with different Burgers vectors $\boldsymbol{b}_1$ and $\boldsymbol{b}_2$ or $\boldsymbol{b}_1$ and $\boldsymbol{b}_3$ (see Fig. 1c). With this assumption, the estimate of $f_1$=0.38 suggests that the length of the ITB fragments containing three adjacent dislocations specified by the zero sum Burgers vector makes up 72% of the total ITB length. This explains the observation of the migration of the ITB with the length $h > h_c$, containing ITB fragments with the zero sum Burgers vector [25].

We now define the critical stress $\tau_c$ as the minimum non-negative stress (for a given twin thickness $h$) at which detwinning via the formation and migration of an ITB is favored at least for some values of the disclination strength $\omega$. In other words, $\tau_c$ corresponds to the minimum value of $\tau'$ (equal to $\tau'(\omega_e)$) at $h \geq h_c$, and $\tau_c = 0$ at $h < h_c$. The dependence of the critical stress $\tau_c$ on twin thickness $h$ for nanotwinned Cu is presented in Fig. 3b. From Fig. 3b it follows that, similar to the equilibrium disclination strength $\omega_e$, the critical stress $\tau_c$ quickly increases with the twin thickness $h$ at $h > h_c$ until $h$ reaches 5–10 nm. After that, $\tau_c$ only slightly increases with increasing $h$. Also, Fig. 3b shows that, if the twin thickness lies in the interval 5–25 nm, the critical shear stress is around 0.7–0.8 GPa. These values are higher than the typical values of the resolved shear stress during the unixial deformation of nanotwinned Cu, but they can be reached at some regions of nanotwinned Cu due to stress concentration or in the regions near the indenter in the case of indenter loading.

## 4. EFFECT OF DETWINNING ON ELECTRIC RESISTIVITY IN ULTRAFINE-GRAINED METALS WITH NANOTWINNED STRUCTURES

Now let us estimate the effect of detwinning on the electrical resistivity of nanotwinned metals. For definiteness, we focus on the case of ultrafine-grained Cu containing ultrathin twins. As is shown in the previous section, in this case, detwinning does not require the action of high stresses and can occur in the whole volume of the nanotwinned solid, resulting in the complete disappearance of the nanotwinned structure.

As a first approximation, the electrical resistivity $\rho$ of a nanotwinned metal can be calculated as [14]

$$\rho = \rho_0 + \rho_{GB} S_{GB} + \rho_{CTB} S_{CTB}, \quad (6)$$

where $\rho_0$ is the resistivity of a metal in the absence of GBs and CTBs, $\rho_{GB}$ is the resistivity of GBs, $\rho_{CTB}$ is the resistivity of CTBs, $S_{GB}$ is the total area of GBs per unit volume, and $S_{CTB}$ is the total area of CTBs per unit volume. The quantities $S_{GB}$ and $S_{CTB}$ can be roughly estimated as $S_{GB} \approx 3/d$ and $S_{CTB} \approx 1/h$, where $d$ is the grain size and $h$ is the twin thickness, as above. After complete detwinning, all the CTBs disappear, and the electrical resistivity $\rho_{detw}$ of a metal can be written as

$$\rho_{detw} = \rho_0 + \rho_{GB} S_{GB}. \quad (7)$$

Comparison of formulae (6) and (7) shows that detwinning, leading to the removal of CTBs, reduces the electrical resistivity and the relative decrease in the resistivity is given by the ratio $(\rho_0 - \rho_{detw})/\rho_0$.

Let us estimate the relative decrease in the resistivity in Cu due to detwinning of the initially nanotwinned solid, for $h$ = 2 nm and various values of grain size $d$. For Cu at room temperature, we have the following estimates [14]: $\rho_0 = 1.69 \times 10^{-8}$

Ohm·m, $\rho_{GB} = 3.6\times10^{-16}$ Ohm·m$^2$, and $\rho_{CTB} = 1.7\times10^{-17}$ Ohm ·m$^2$. Then for $d$ = 100, 200, and 300 nm, we obtain: $(\rho_0 - \rho_{detw})/\rho_0$=0.235, 0.276, and 0.293, respectively. This implies that complete detwinning of ultrafined-grained nanotwinned Cu with ultrathin twins results in a decrease of its electrical resistivity by 20-30%.

## 5. CONCLUDING REMARKS

Thus, in this paper, we have suggested a theoretical model describing a plastic deformation mode – the detwinning processes that occur through stress-driven migration of ITBs (Fig. 1) – in nanotwinned metals. In doing so, detwinning of a nanoscale twin is viewed as a deformation process carried by a dipole of wedge disclinations located at the junctions of incoherent and coherent twin boundaries (Fig. 1d). The strength magnitude $\omega$ of such disclinations specifies plastic shear associated with detwinning.

Within the suggested model, the stress characteristics of the detwinning processes in nanotwinned metals with fcc crystal lattices are calculated. In particular, the critical external stress $\tau'$ (for athermal migration of an incoherent boundary of a nanoscale twin and the associated twin shrinkage) is revealed as a function of the disclination strength w (Fig. 2). With the dependence $\tau'(\omega)$ calculated at the twin thickness $h$ = 2 nm (Fig. 2b), it is found that the formation and migration of the incoherent boundaries of ultrathin nanotwins (characterized by $h < h_c$, where the critical twin thickness $h_c \approx 2.2$ nm for Cu) is favored even in the situation with $\omega = 0$, corresponding to the zero net Burgers vector of the ITB. This result is well consistent with the experimental observation [26] of the motion of an ITB containing a dislocation array characterized by a zero net Burgers vector in nanotwinned Cu under indenter loading in the case of twin thickness being around 2 nm.

Also, it is found that in the case of ultrathin twins, the detwinning process is energetically favored even in the situation where the external stress is absent. In this situation, the release of the energy of coherent twin boundaries (that disappear when the detwinning process comes into play) serves as the driving force for migration of ITBs (Fig. 1).

Finally, we have estimated the effect of the detwinning processes on the electric resistivity of nanotwinned Cu with ultrathin twins. It has been demonstrated that complete detwinning of ultrafine-grained Cu that initially contains ultrathin twins can reduce its resistivity by 20 to 30%, thus enhancing its conducting properties.

## ACKNOWLEDGEMENTS

This work was supported, in part (for IAO), by the Ministry of Education and Science of Russian Federation (Grant 14.B25.31.0017), in part (for NVS), by the Ministry of Education and Science of Russian Federation (Zadanie № 9.1964.2014/K) and St. Petersburg State University (research grant 6.37.671.2013), in part (for AGS), by the Ministry of Education and Science of Russian Federation (grant MD-2893.2015.1) and the Russian Fund of Basic Research (grant 15-31-20095).

## REFERENCES

[1] R.Z. Valiev and T.G. Langdon // *Progr. Mater. Sci.* **51** (2006) 881.
[2] M. Kawasaki and T.G. Langdon // *J. Mater. Sci.* **42** (2007) 1782.
[3] R.Z. Valiev, I. Sabirov, A.P. Zhilyaev and T.G. Langdon // *JOM* **64** (2012) 1134.
[4] Y. Estrin and A. Vinogradov // *Acta Mater*. **63** (2013) 782.
[5] I.A. Ovid'ko and A.G. Sheinerman // *Rev. Adv. Mater. Sci.* **37** (2014) 97.
[6] A.P. Zhilyaev, S.N. Sergeev, V.A. Popov and A.V. Orlov // *Rev. Adv. Mater. Sci.* **39** (2014) 15.
[7] A.A. Samigullina, A.A. Nazarov, R.R. Mulyukov, Yu.V. Tsarenko and V.V. Rubanik // *Rev. Adv. Mater. Sci.* **39** (2014) 48.
[8] R.K. Islamgaliev, V.D. Sitdikov, K.M. Nesterov and D.L. Pankratov // *Rev. Adv. Mater. Sci.* **39** (2014) 61.
[9] I.A. Ovid'ko and A.G. Sheinerman // *Rev. Adv. Mater. Sci.* **39** (2014) 9.
[10] I.A. Ovid'ko and A.G. Sheinerman // *Rev. Adv. Mater. Sci.* **39** (2014) 99.
[11] L. Lu, X. Chen, X. Huang and K. Lu // *Science* **323** (2009) 607.
[12] K. Lu, L. Lu and S. Suresh // *Science* **324** (2009) 349.
[13] Y.M. Wang, F. Sansoz, T. LaGrange, R.T. Ott, J. Marian, T.W. Barbee Jr. and A.V. Hamza // *Nature Mater*. **12** (2013) 697.
[14] L. Lu, Y. Shen, X. Chen, L. Qian and K. Lu // *Science* **304** (2004) 422.
[15] T. Zhu and H. Gao // *Scr. Mater.* **66** (2012) 843.
[16] Z. You, X. Li, L. Gui, Q. Lu, T. Zhu, H. Gao and L. Lu // *Acta Mater.* **61** (2013) 217.
[17] Q. Huang, D. Yu, B. Xu, W. Hu, Y. Ma, Y. Wang, Z. Zhao, B. Wen, J. He, Z. Liu and Y. Tian // *Nature* **510** (2014) 250.

[18] P. Gu, M. Dao and Y. Zhu // *Philos. Mag.* **94** (2014) 1249.
[19] H. Zhou, X. Li, S. Qu, W. Yang and H. Gao // *Nano Lett.* **14** (2014) 5075.
[20] N.F. Morozov, I.A. Ovid'ko and N.V. Skiba // *Rev. Adv. Mater. Sci*. **37** (2014) 29.
[21] I.A. Ovid'ko, A.G. Sheinerman and N.V. Skiba // *Rev. Adv. Mater. Sci*. **41** (2015) 93.
[22] X. Li, Y. Wei, L. Lu, K. Lu and H. Gao // *Nature* **464** (2010) 877
[23] Z. You, X. Li, L. Gui, Q. Lu, T. Zhu, H. Gao and L. Lu // *Acta Mater.* **61** (2013) 217.
[24] Y. Tian, B. Xu, D. Yu, Y. Ma, Y. Wang, Y. Jiang, W. Hu, C. Tang, Y. Gao, K. Luo, Z. Zhao, L.-M. Wang, B. Wen, J. He and Z. Liu // *Nature* **493** (2013) 385.
[25] J. Wang, N. Li, O. Anderoglu, X. Zhang, A. Misra, J.Y. Huang and J.P. Hirth // *Acta Mater.* **58** (2010) 2262.
[26] N. Li, J. Wang, J.Y. Huang, A. Misra and X. Zhang // *Scr. Mater.* **64** (2011) 149.
[27] Y. Liu, J. Jian, Y. Chen, H. Wang and X. Zhang // *Appl. Phys. Lett.* **104** (2014) 231910.
[28] N. Lu, K. Du, L. Lu and H. Q. Ye // *J. Appl. Phys.* **115** (2014) 024310.
[29] Y. Liu, N. Li, D. Bufford, J. H. Lee, J. Wang, H. Wang and X. Zhang // *JOM* (2015) (DOI: 10.1007/s11837-015-1518-1).
[30] M.Yu. Gutkin, K.N. Mikaelyan, A.E. Romanov and P. Klimanek // *Phys. Status Solidi* A **193** (2002) 35.
[31] R. Niu and K. Han // *Scr. Mater.* **68** (2013) 960.